data

MDPI

Data Descriptor

A Curated Dataset of Regional Meteor Events with Simultaneous Optical and Infrasound Observations (2006–2011)

Elizabeth A. Silber [1,*], Emerson Brown [1,2,†], Andrea R. Thompson [1,3,†] and Vedant Sawal [1]

[1] Sandia National Laboratories, 1515 Eubank Blvd. NE., Albuquerque, NM 87123, USA
[2] Department of Physics and Astronomy, Northwestern University, 2145 Sheridan Rd., Evanston, IL 60208, USA
[3] Department of Geology, Central New Mexico Community College, 900 University Blvd SE, Albuquerque, NM 87106, USA
* Correspondence: esilbe@sandia.gov
† Contributions made as part of a summer internship at Sandia National Laboratories.

Abstract

We present a curated, openly accessible dataset of 71 regional meteor events simultaneously recorded by optical and infrasound instrumentation between 2006 and 2011. These events were captured during an observational campaign using the all-sky cameras of the Southern Ontario Meteor Network and the co-located Elginfield Infrasound Array. Each entry provides optical trajectory measurements, infrasound waveforms, and atmospheric specification profiles. The integration of optical and acoustic data enables robust linkage between observed acoustic signals and specific points along meteor trajectories, offering new opportunities to examine shock wave generation, propagation, and energy deposition processes. This release fills a critical observational gap by providing the first validated, openly accessible archive of simultaneous optical–infrasound meteor observations that supports trajectory reconstruction, acoustic propagation modeling, and energy deposition analyses. By making these data openly available in a structured format, this work establishes a durable reference resource that advances reproducibility, fosters cross-disciplinary research, and underpins future developments in meteor physics, atmospheric acoustics, and planetary defense.

Dataset: https://doi.org/10.5281/zenodo.15868512.

Dataset License: CC-BY-NC

Keywords: meteoroids; meteors; fireballs; infrasound; astrometry; atmospheric acoustics; shock waves; multi-sensor dataset; planetary defense; atmospheric entry

Academic Editor: Milan S. Dimitrijević

Received: 29 July 2025
Revised: 21 August 2025
Accepted: 27 August 2025
Published: 28 August 2025

Citation: Silber, E.A.; Brown, E.; Thompson, A.R.; Sawal, V. A Curated Dataset of Regional Meteor Events with Simultaneous Optical and Infrasound Observations (2006–2011). *Data* **2025**, *10*, 138. https://doi.org/10.3390/data10090138

1. Summary

1.1. Background

This dataset provides a curated, open-access archive of 71 regional meteor events simultaneously observed using optical and infrasound instrumentation [1,2]. The events were originally recorded between 2006 and 2011 as part of a multi-year observational campaign led by the Western Meteor Physics Group (WMPG) in the Department of Physics and Astronomy, Western University in London, Ontario, Canada. Each event was simultaneously detected by the all-sky optical cameras, which are part of the Southern Ontario Meteor Network (SOMN), and the Elginfield Infrasound Array (ELFO), a four-element acoustic array located nearby [3]. These coincident detections present a rare opportunity

to study multi-sensor signatures of meteoroids entering the atmosphere at hypersonic velocities and generating low-frequency acoustic energy (<20 Hz) via shock wave formation. Some meteors had more than one infrasound detection, bringing the number of total acoustic detections to 90.

The dataset stems from the events analyzed in the study by Silber, et al. [2] titled "*Optical Observations of Meteors Generating Infrasound—I: Acoustic Signal Identification and Phenomenology*". That foundational paper characterized the relationship between luminous and acoustic signals using these events, but it did not release the complete underlying raw data in a structured or publicly accessible format. We also note that a smaller subset of these events was also analyzed by Edwards et al. [3] in an earlier study. The present work addresses that gap by consolidating raw measurements and derived parameters across all available modalities into a consistent and reusable archive. The complete dataset, including all 71 events and supporting summary tables, is archived and openly available at Zenodo.

The dataset spans the years 2006–2011, reflecting the timeframe of a specific observational project during which validated, simultaneous optical and infrasound detections were systematically analyzed and documented. Although both the SOMN and ELFO have continued operations beyond 2011, no further validated coincident datasets of this scope were produced. Should future studies of comparable design be undertaken, we strongly encourage that their datasets likewise be curated and openly released.

1.2. Value of the Data

The curated meteor dataset presented here offers several significant benefits to the scientific community, a subset of which is briefly summarized below. These examples represent only a fraction of the potential applications; the dataset is intentionally structured to support diverse and unforeseen uses across disciplines.

- Multi-sensor linkage at regional distances: This dataset uniquely captures a structured set of regional meteor events simultaneously recorded by optical and infrasound sensors. The proximity of these meteors (within approximately 300 km of the infrasound detection array) preserves acoustic signal characteristics by minimizing propagation-related distortions [2,3], thus retaining original source properties and reducing atmospheric propagation uncertainties [4,5].
- High-fidelity ground-truth for modeling and validation: The dataset supports empirical evaluation of trajectory reconstruction algorithms [6–8], period–energy scaling relationships [9–12], and propagation modeling of meteor-generated infrasound [13]. The availability of high-fidelity astrometric and photometric data enables independent derivation of entry parameters that are critical for interpreting acoustic signatures [14–17].
- Publicly accessible and curated for reuse: All files are organized into standardized folders and subfolders for each event, with consistent naming, metadata, and open formats. The archive includes trajectory solutions, time-synchronized infrasound waveforms, calibrated astrometry, and atmospheric specifications needed to perform propagation modeling. This structured design supports straightforward reuse in atmospheric science, planetary defense, meteor physics, and signal-processing domains.
- Relevance to planetary defense and acoustic monitoring: The dataset captures meteor events that are too small, too frequent, or too low-energy to be reliably detected by satellite systems or distant infrasound stations. It serves as a benchmark resource for short-range infrasound detection capability (<300 km) and for testing signal discrimination methods used in acoustic monitoring frameworks.

We emphasize that this paper does not provide new scientific analysis of meteor behavior; rather, it describes the curated dataset in detail and makes it openly accessible. Readers interested in the physical interpretation of these events should consult previously

published analyses (e.g., [2,18,19]), while the present work ensures that the underlying observational data are available for independent analysis and reuse.

2. Context and Novelty of This Curated Release

The purpose of this paper is to document and release the dataset in a structured and reusable format, consistent with FAIR principles. It is intended as a reference data resource rather than an analytical study of meteor entry behavior. Although the events in this dataset have been analyzed in prior studies [1–3,19], those investigations emphasized scientific interpretation rather than systematic data dissemination. The fundamental observational data, including original waveform records, astrometric solutions, atmospheric specifications, and derived trajectory parameters, were previously either stored locally, archived in heterogeneous formats, or presented only partially in limited tabular summaries. To date, no comprehensive, unified, and openly accessible dataset has been assembled or released for these events.

The dataset presented here addresses this gap by offering a curated, openly accessible archive of 71 regional meteor events simultaneously recorded by optical and infrasound instrumentation. Data from each meteor event have been consolidated systematically, incorporating both raw measurements and processed results into structured directories designed for reproducibility and independent verification. The optical component comprises original astrometric imagery, derived trajectory solutions, and, where applicable, photometric light curves. Corresponding acoustic data include waveform recordings presented in multiple formats. Additionally, event-specific atmospheric specification profiles are provided when available, facilitating propagation modeling efforts.

In addition to standardized data formats, the dataset provides consistent temporal and spatial associations between optical and acoustic measurements. This coherent integration facilitates subsequent research into sensor fusion methods, trajectory reconstruction techniques, and meteoroid energy estimation. In contrast to prior analyses primarily concerned with scientific interpretation, such as acoustic signal classification or detection phenomenology, this dataset explicitly serves as a comprehensive community resource. It has been purposefully structured to facilitate modeling, simulation, and validation tasks within atmospheric acoustics and meteoroid physics research domains.

Consequently, this archival effort significantly advances the value and usability of data derived from this observational campaign, preserving original data fidelity, increasing discoverability, and providing sustained, long-term accessibility consistent with FAIR (Findable, Accessible, Interoperable, and Reusable) principles. To our knowledge, this represents the most comprehensive publicly available archive of regional meteor events observed simultaneously by calibrated optical and infrasound instrumentation.

3. Data Description

All data described in this section are available in full at Zenodo (https://doi.org/10.5281/zenodo.15868512), where the curated archive provides both raw observational files and consolidated summary tables. The curated dataset presented here is organized and structured to facilitate straightforward access, reproducibility, and interoperability. Each meteor event has a dedicated directory named according to its detection time, formatted as yyyymmdd_hhmmss. This naming convention corresponds to the UTC date and time of the observed meteor event, where: ‘yyyy’ refers to the four-digit year of detection, ‘mm’ represents the two-digit month (01–12), ‘dd’ denotes the two-digit day of the month (01–31), ‘hh’ indicates the two-digit hour (00–23), ‘mm’ specifies the two-digit minute (00–59), and ‘ss’ refers to the two-digit second (00–59). For example, an event recorded at 04:15:22 UTC on 5 August 2007, is labeled 20070805_041522. There are 71 distinct meteor events, and therefore

71 event-specific folders. Of these, 55 had a single infrasound detection, and the remainder had two or more detections, bringing the total number of acoustic signatures to 90.

The dataset contains the following directories and file types: (i) Infrasound data; (ii) optical observations data; (iii) atmospheric specification data; (iv) consolidated tables, and (v) README files. Additionally, each primary data group (infrasound data, optical data, atmospheric profiles) has its own dedicated README file describing data formats, contents, and recommended usage. The hierarchical structure of these data types and their relationships within the dataset are illustrated in Figure 1. This archive provides complete astrometric data, acoustic waveform recordings, and atmospheric specification profiles for all events. Full photometric information is available only for a subset of events; while some include derived light curves, others do not. Consequently, photometric data are provided with variable completeness across the 71 events. Updating the photometric record to achieve full coverage is not feasible within the scope of this effort; the objective is to release the validated data currently available in a consistent, FAIR-compliant format.

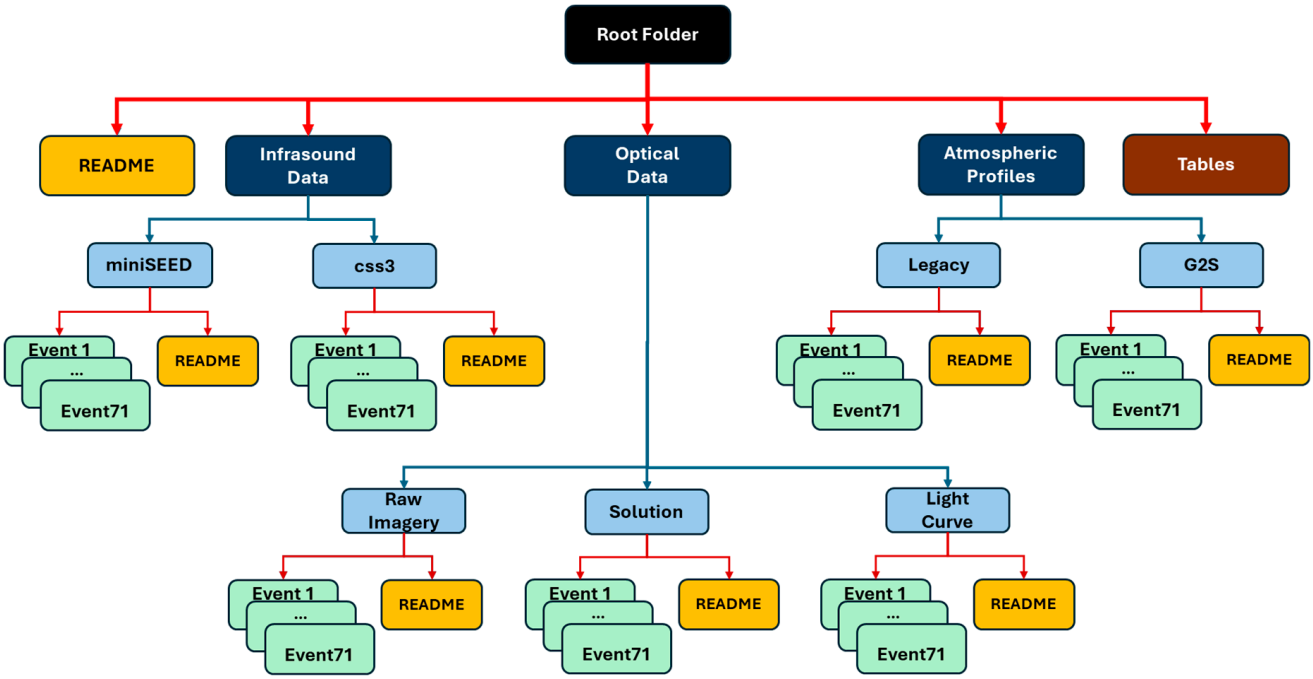

Figure 1. Schematic illustration of the dataset folder structure, showing the hierarchical organization of primary data categories: infrasound waveform data, optical observations, atmospheric specification profiles, consolidated summary tables, and README documentation files. Each primary category contains distinct subdirectories for ease of navigation and analysis. Each primary data group (infrasound data, optical data, atmospheric profiles) contains its own dedicated README file, describing data formats, contents, and recommended usage to facilitate effective dataset navigation and analysis.

3.1. Infrasound Data

Infrasound data recorded by ELFO [2,3] are provided in two widely utilized and standardized waveform formats:

i. CSS3 (Center for Seismic Studies Version 3) format: Standard seismic/infrasound data representation including waveform files (.w), waveform description files (.wfdisc), and sensor site files (.site). These files are compatible with standard seismic and acoustic data processing software packages, such as ObsPy[1] [20–22].

ii. miniSEED (mini Standard for the Exchange of Earthquake Data) format: Standard data-exchange format used widely within the seismic and acoustic community, en-

suring compatibility with major analysis software suites such as ObsPy[2] [20–22]. The miniSEED data for ELFO are freely available to download from Natural Resources Canada (NRCAN)[3], a member of the International Federation of Digital Seismograph Networks (FDSN). The network code is CN.

These waveform data capture the raw acoustic signals, preserving original sampling rates and timing metadata needed for robust acoustic signal analysis and validation.

3.2. Optical Observations Data

The astrometry data for each event are organized into dedicated subdirectories. These include

i. Raw astrometric imagery: Original video frames or image files capturing the meteor from multiple camera stations.
ii. Astrometric solutions: Files containing trajectory solutions, typically provided in tabular format with information such as time, azimuth, elevation, and geographic coordinates.
iii. Light curves (if available): Brightness profiles in text-based or tabular form, documenting meteor luminosity evolution along the observed trajectory. Approximately 32% of events have light curves because a subset of events was post-processed to that extent. These mainly stem from a follow-on publication that presented detailed weak shock and modeling analyses [19].

Astrometric data provided in this structured manner allow users to independently derive and verify trajectory solutions, investigate meteor fragmentation events, and correlate luminosity data directly with recorded acoustic waveforms. In terms of full photometric information, of the 71 meteors, 23 include derived light curves (~32% of the dataset), while the remainder do not. This variability reflects the extent of prior photometric reduction efforts.

Some raw astrometric imagery directories contain dump*.png images, which are sequential diagnostic frames generated by the original reduction software. Individual frames are included for all events, though the file naming convention varies with the processing pipeline. For 2006–2007 events, both frame*.png and dump*.png appear depending on how the event was reduced, while from 2008 onward, all events use dump*.png. Both formats represent sequential frame records of meteor trajectories. Each frame image includes an embedded timestamp and camera number, allowing direct correlation with the event and metadata. The presence of dump versus frame filenames therefore reflects changes in the original processing workflow.

In addition to the curated astrometric and trajectory products, the archive also contains a number of intermediate and diagnostic files generated by the original reduction workflow. These files were designed for internal use, are not formally standardized, and in some cases may lack axis labels or detailed headers. They are preserved here to maintain completeness of the record but are not required to use the dataset. For example, the associated ancillary calibration products, such as mask.png and dark.png (when available), are included to preserve completeness of the archive but are not required to use the dataset. Concise documentation is provided in the accompanying READMEs, and for specialized file types originating from legacy workflows, users are referred to WMPG publications for further detail (e.g., [23–27]).

3.3. Atmospheric Specification Profiles

Accurate atmospheric specifications are essential for reliable acoustic propagation modeling. For each meteor event, two types of atmospheric data are provided:

i. Legacy atmospheric specifications: These profiles are derived from a combination of assimilated atmospheric temperature and wind data provided by the United Kingdom Meteorological Office (UKMO) [28], merged with high-altitude wind fields from the Horizontal Wind Model (HWM) [29], following methodologies previously documented by Silber, et al. [2]. We include two formats, .txt and .csv (comma separated values). The data columns include geopotential height (km), temperature (K), zonal (u) and meridional (v) wind components (m/s), and atmospheric pressure (mbar or hPa). The profiles are generated for the geographic location of ELFO (43.19° N, −81.31° E) and correspond specifically to the hour of each meteor event. The original publication exclusively employed the legacy atmospheric specifications.
ii. G2S (Ground-2-Space): Atmospheric specifications hosted by the National Center for Physical Acoustics (NCPA) [30]. G2S is a model combining ground-level observational data and upper atmospheric specifications from space-based measurements and numerical weather prediction models [5]. The profiles include temperature (K), zonal (positive eastward) (u) and meridional (positive northward) (v) components of wind velocity (m/s), atmospheric pressure (mbar), and density (g/cm^3) data at intervals of one hour or greater for the entire day of the event, depending on data availability. These profiles have been widely used to model infrasound propagation and are standard within the acoustic modeling community [5,30–32]. While not employed in the original study, these G2S profiles are included here to provide end-users with additional atmospheric data products that may prove beneficial for future research, modeling, or validation activities. Each atmospheric profile corresponds to the geographic location of ELFO (43.19° N, −81.31° E).

3.4. Consolidated Data Tables

To enable rapid overview and access, consolidated tables summarizing a series of parameters from both optical and acoustic datasets are provided. These consolidated data tables include

i. Infrasound signal summary: A comprehensive summary table listing event timestamps, acoustic waveform durations, amplitudes, dominant frequencies, celerities, arrival azimuths, and many other measurements, all of which are described in the associated README files (see Section 3.5).
ii. Astrometric summary: A consolidated table containing event timestamps, trajectory start and end coordinates, velocities, orbital parameters, and many other entries, all of which are described in the associated README files (see Section 3.5).

These tables allow quick reference and selection of events based on primary observational parameters, aiding users in selecting specific subsets of data for detailed investigations or modeling activities. Each column contains the explicitly defined label and units, enabling clear identification of the parameter(s) of interest. Moreover, the list of all parameters is available in the associated README files.

3.5. README Files

Each primary data category (Infrasound data, Optical data, and Atmospheric specification profiles) includes dedicated README files. These plain-text README files provide detailed explanations about data formats, file naming conventions, content descriptions, data-processing notes, and suggested methodologies for data analysis and interpretation. A general README file provided at the root directory summarizes the overall dataset structure, offers guidance on event selection and navigation, and defines key metadata parameters.

To further assist users in efficiently utilizing the dataset, a User Manual in PDF format is made available. This User Manual integrates all README content and provides a description of the dataset's file and directory structure.

4. Physical Context: Meteoroid Entry, Shock Generation, and Acoustic Observations

Effective interpretation of meteor-generated infrasound requires an understanding of the fundamental processes governing meteoroid entry, atmospheric shock generation, and the resulting acoustic signatures [33]. The following subsections provide this physical context as a framework for using the dataset, enabling users to interpret, validate, and apply the observations in modeling, simulation, and theoretical studies.

4.1. Meteor Entry Physics and Shock Formation

Meteoroids enter Earth's atmosphere at hypersonic velocities ranging from 11.2 to 72.8 km/s [34]. As they penetrate the progressively denser atmospheric layers, rapid energy transfer occurs through aerodynamic interactions, leading to intense heating and ablation of meteoroid surface layers [35]. The luminous phenomenon resulting from this process is commonly observed as a meteor [34]. The associated release of kinetic energy produces shock waves that propagate outward from the meteoroid trajectory [33,36,37]. The detailed theoretical framework describing these processes, including aerodynamic heating, shock wave physics, and fragmentation mechanisms, has been extensively documented in previous studies [33,38,39].

Shock waves arise from rapid energy deposition during hypersonic passage. They are broadly categorized as cylindrical (ballistic) or spherical (point-source) [18,38,40,41]. Cylindrical shocks result from continuous ablation along the trajectory, radiating acoustic energy mainly perpendicular to the path [42]. Spherical shocks, by contrast, stem from discrete fragmentation episodes, often observed as bright flares [34], and radiate more omnidirectionally [18,43].

4.2. Optical Observations and Trajectory Reconstruction

Accurate meteor trajectory solutions derived from optical astrometric observations are fundamental for interpreting meteor-generated acoustic signals [2,25,41]. In particular, distinguishing cylindrical from spherical shock sources depends directly on the reliability of optical trajectory determinations. Prior studies e.g., [2] have described the methodology in detail and demonstrated the necessity of robust trajectory reconstruction for confident source characterization.

Multi-sensor data integration allows robust testing and advancement of models related to atmospheric acoustics, shock wave physics, and meteoroid entry dynamics, serving as a foundational resource for both empirical investigations and theoretical modeling efforts within these research domains. High-quality optical measurements of meteors using ground-based all-sky camera systems enable accurate trajectory reconstruction [25–27]. Figure 2 illustrates the geometry of a meteor event observed by multiple all-sky cameras. Triangulated measurements yield trajectories that, when correlated with brightness variations, allow identification of fragmentation points. These provide essential context for interpreting associated acoustic signals.

4.3. Acoustic Detection

Acoustic signals generated by meteors propagate through the atmosphere as low-frequency pressure waves or infrasound (<20 Hz) [44]. These signals can be detected at ground-based arrays positioned regionally (<300 km) from the meteor entry path. At such

short distances, acoustic propagation occurs primarily along direct paths, with limited influence from atmospheric ducting and scattering [2,45].

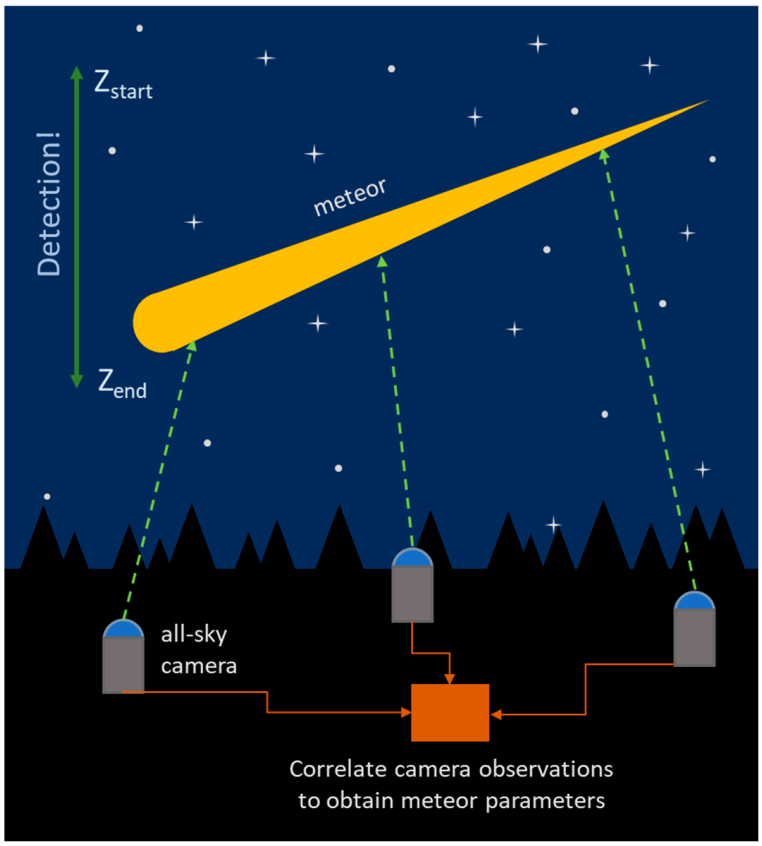

Figure 2. Diagram illustrating optical detection of a meteoroid event using a network of all-sky cameras. Each station simultaneously records the luminous trajectory of the meteor from its initial detection altitude (Z_{start}) to its final altitude (Z_{end}). The luminosity onset and terminal altitudes can vary significantly depending on entry speed, angle, composition, and size. Correlation of multi-station observations enables accurate determination of trajectory geometry, velocity, and photometric evolution, forming the basis for dynamic and photometric characterization.

Figure 3 shows a schematic representation of cylindrical shock generation and acoustic detection. The expanding cylindrical wavefront illustrates how pressure disturbances propagate from the meteor trail to regional arrays [33,37,42]. Ground-based arrays record resulting pressure fluctuations, enabling extraction of fundamental signal parameters, including arrival direction, source altitude, dominant acoustic frequency, and signal duration e.g., [43]. The figure is not to scale and does not attempt to represent all physical processes in detail. In particular, fragmentation-generated spherical shocks are not shown, as these have been addressed extensively in prior studies (e.g., [18,33,37]). In real events, fragmentation introduces additional spherical shock sources that complicate the acoustic radiation pattern.

4.4. Importance of Integrated Optical and Acoustic Data

Integrating optical and acoustic measurements provides powerful advantages for interpreting meteoroid entry phenomena. Optical observations deliver accurate positional and timing information, while acoustic measurements characterize energy deposition and shock source properties. Prior studies (e.g., [2,14,43]) have demonstrated that combining these modalities enables robust discrimination between cylindrical and spherical shocks and facilitates accurate determination of acoustic source altitudes. Such integration also serves as a foundational approach for validating shock physics theories, refining atmo-

spheric acoustic propagation models, and informing planetary defense applications. By offering multi-sensor datasets, this archive supports rigorous testing of models that link meteoroid dynamics, shock generation, and acoustic signatures, thereby serving as a lasting resource for both empirical investigations and theoretical research.

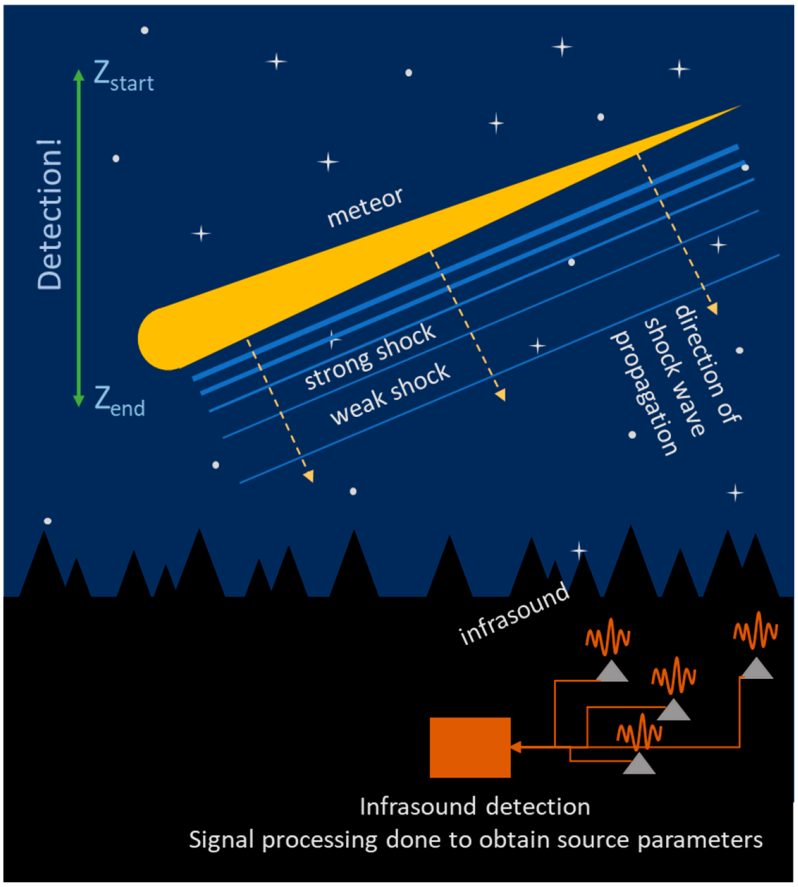

Figure 3. Schematic representation of infrasound detection from a meteoroid generating a cylindrical shock wave along its atmospheric path. Acoustic energy propagates as an expanding wavefront, with signal strength modulated by shock strength and fragmentation events. This figure is intended as a conceptual illustration of geometry and workflow rather than a physical model; fragmentation episodes and associated spherical shocks are not depicted here, as these processes are discussed in detail elsewhere (e.g., [18,33,37]). Infrasound arrays record resulting pressure fluctuations, which are then processed to extract source parameters including altitude, dominant frequency, and propagation direction. Note: This diagram represents an idealized scenario without fragmentation.

4.5. Scope and Selection of Events in This Dataset

The meteoroid events presented in this dataset do not encompass all simultaneous optical–acoustic detections from the observational campaign. Instead, they represent a carefully curated subset of regional events (within ~300 km of the observing array), selected for the exceptional completeness and quality of their multi-sensor records. Selection criteria included robust multi-station optical astrometry, clear acoustic signal detections, and reliable temporal and spatial correlations between optical trajectories and acoustic waveforms. The resulting dataset thus captures the best-documented cases from the campaign, providing a comprehensive empirical resource suitable for subsequent investigations of meteor physics, atmospheric acoustics, and related modeling efforts.

5. Geographical Context and Instrumentation

5.1. Observational Region and Institutional Context

The observational data described here were recorded in Southwestern Ontario, Canada, centered around Western University in London, Ontario (also known as the University of Western Ontario or UWO). The location of the observational campaign therefore directly resulted from the presence of Western University, where both the SOMN all-sky camera network and the Elginfield Infrasound Array are managed and operated [3,23,25–27].

WMPG's established research infrastructure and expertise in meteor physics and atmospheric acoustics made this region a logical and suitable environment for simultaneous optical and infrasound meteor observations. Figure 4 provides a geographic overview, showing the positions of the SOMN camera stations (red circles) and the ELFO array (yellow triangle, coinciding with the location of the Elginfield camera) in the Southwestern Ontario region. Western University, which facilitated efficient maintenance, calibration, and coordination throughout the observational period, is located in London, Ontario, Canada (43.0096° N, −81.2737° E). This arrangement allowed effective overlapping coverage and direct propagation paths, critical for accurate trajectory reconstruction and acoustic signal association.

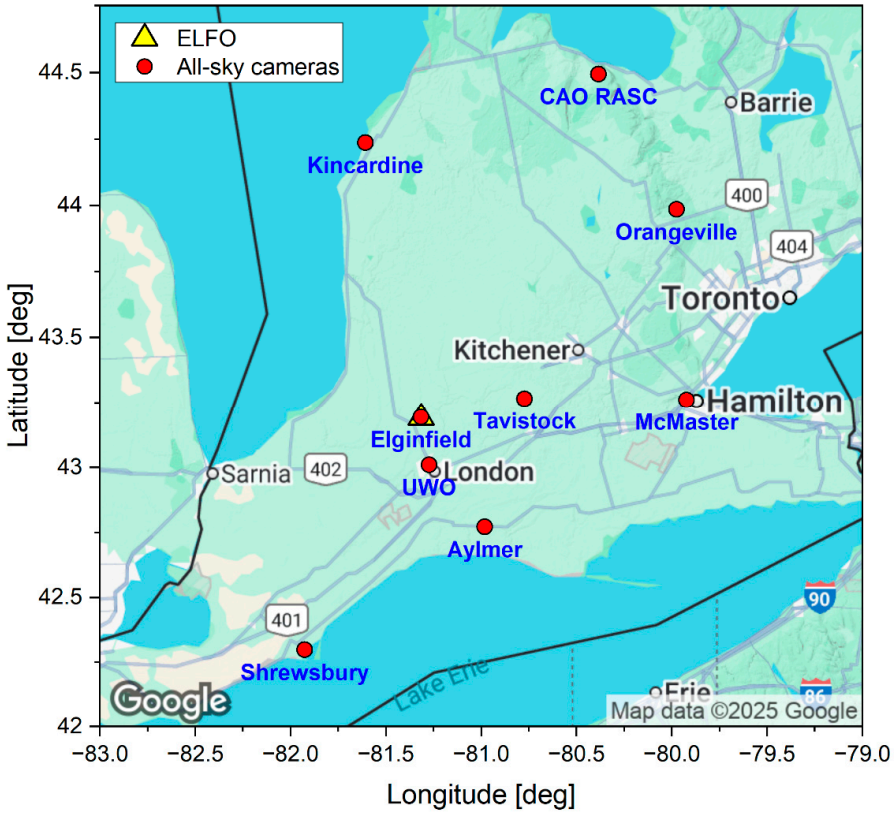

Figure 4. Geographic overview of the SOMN optical camera stations (red circles) and ELFO (yellow triangle). The map extent shown in this figure covers approximately 325 km east–west and 280 km north–south. Background map from Google Earth, © Google.

5.2. Optical Camera Network Configuration

The optical component of the observational network consists of multiple automated all-sky camera systems deployed across Southwestern Ontario as part of SOMN, operated by the Western Meteor Physics Group (WMPG) at Western University [23,25]. These camera stations continuously monitor the night sky to record bright meteors (fireballs) as they enter and ablate within Earth's atmosphere. Each station uses sensitive, low-light video

cameras equipped with wide-angle lenses to ensure maximum sky coverage. Cameras are housed within protective enclosures fitted with transparent acrylic domes, designed to withstand environmental conditions while minimizing optical distortions. Environmental controls inside the enclosures, including thermostatically controlled heaters and circulation fans, maintain clear optical conditions by reducing condensation and frost formation. Additionally, ambient-light sensors automatically power down camera systems during daylight hours, thus conserving operational lifespan and data storage.

Meteor events captured by these cameras are recorded in a digital video format at approximately 30 frames per second, providing adequate temporal resolution for accurate determination of meteor trajectories and velocities. Frame-grabbing hardware within dedicated computer systems digitizes and processes incoming video streams for subsequent analysis. Real-time meteor detection and processing are handled by the All-Sky Guided Automatic Real-Time Detection (ASGARD) software, developed by WMPG. Early versions of this software and related data-reduction methodologies were initially described by Weryk, et al. [24]. ASGARD software detects meteors as they appear in real time within the video stream, capturing and storing associated data for subsequent astrometric and photometric analysis. The software operates under the Debian GNU/Linux environment and accommodates various video input types, including analog camera feeds, pre-recorded digital video, and digital camera interfaces. Timing information, essential for accurate trajectory reconstruction, is maintained by continuously synchronizing camera systems with Global Positioning System (GPS) based timing sources using the Network Time Protocol (NTP). Rather than periodically adjusting system clocks, NTP dynamically adjusts clock rates, consistently maintaining timing accuracy to within one video frame or better.

This standardized and automated observational methodology provides reliable and reproducible meteor observations, facilitating accurate triangulation-based determination of meteor paths, entry velocities, and fragmentation points. Detailed information on camera deployment strategies, data-reduction methodologies, and software development history is thoroughly documented in previous foundational studies [23,24].

5.3. Infrasound Array Configuration

The Elginfield Infrasound Array, also known as ELFO, is owned by NRCAN and operated by Western University. It comprises four Chapparal [46] infrasound sensors arranged in a tripartite configuration optimized for regional-scale detection of meteor-generated acoustic signals [1–3]. Each sensor is situated inside an insulated concrete vault to protect it from elements and reduce temperature fluctuations. To minimize local wind noise [47,48], porous garden hoses, each 15 m in length, are installed and arranged in a star pattern. ELFO4 (northwestern element), however, features a wind shelter, which was built in November 2007. Additionally, snow fences are installed around all elements to further minimize local noise. The array layout was designed to provide measurements of infrasound signal arrival times, back-azimuth directions, and acoustic wave parameters, enabling effective discrimination and characterization of meteor-related acoustic events. The location of the ELFO array (43.1907° N, −81.3152° E, 322 m), approximately 20 km north of Western University, was carefully selected to reduce background acoustic noise levels, thus improving the sensitivity and reliability of infrasound detections. Comprehensive descriptions of array design and signal-processing methodologies employed at ELFO have been thoroughly documented in previous studies [1–3] and are therefore not provided here. Figure 5 provides a schematic representation of the ELFO array configuration, illustrating the relative positions of individual acoustic sensors within the array geometry.

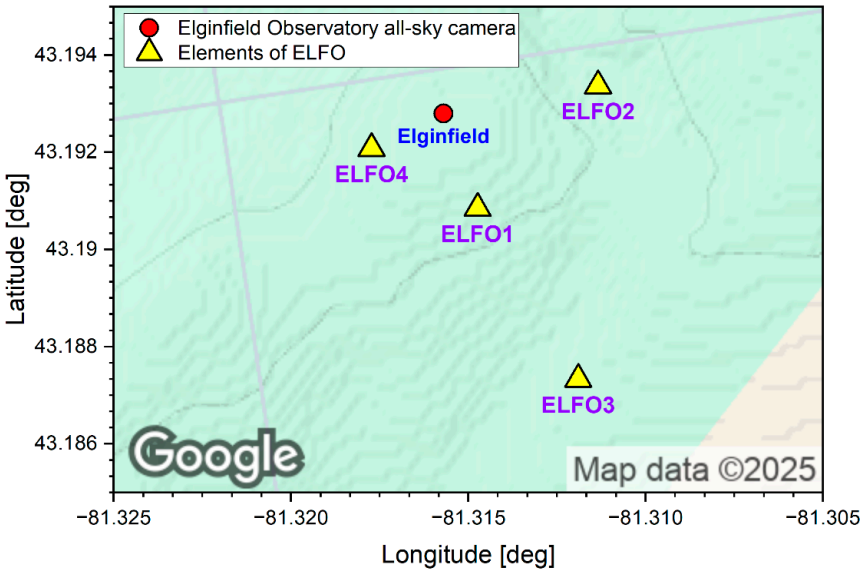

Figure 5. Layout of ELFO showing the relative positions of its four acoustic sensors (yellow triangles). The co-located Elginfield all-sky camera station, part of the SOMN network, is indicated by a red circle. This close arrangement facilitates simultaneous optical and acoustic measurements. The map extent shown in this figure covers ~1.6 km east–west and ~1 km north–south. Background map from Google Earth, © Google.

6. Summary and Conclusions

In this paper, we have presented a curated dataset of 71 regional meteor events recorded simultaneously by optical and acoustic (infrasound) instrumentation. Spanning observations from 2006 to 2011, the dataset includes optical detections, associated infrasound waveforms, and relevant atmospheric specification profiles. Each event was selected for its quality, completeness, and internal consistency, ensuring that the archive provides a robust foundation for subsequent analyses. By combining optical trajectory solutions with acoustic signal recordings, the dataset advances the interpretability of meteor-generated infrasound, enabling detailed examination of shock wave generation processes and supporting rigorous validation of meteor entry, atmospheric propagation, and fragmentation models. Beyond its immediate applications to meteor physics, atmospheric acoustics, and planetary defense, this resource exemplifies the enduring value of open, rigorously curated data as a foundation for reproducible science and future innovation. We encourage future investigations across the sciences to adopt similar practices of releasing comprehensive datasets alongside their analyses, thereby advancing transparency, accelerating discovery, and ensuring that today's observations remain a lasting resource for tomorrow's innovations.

Author Contributions: Conceptualization, methodology, validation, formal analysis, investigation, resources, writing—original draft preparation, visualization, project administration, E.A.S. Data curation, writing—review and editing, all authors contributed. All authors have read and agreed to the published version of the manuscript.

Funding: This work was: in part, supported by the Laboratory Directed Research and Development (LDRD) program (project number 229346) at Sandia National Laboratories, a multi-mission laboratory managed and operated by National Technology and Engineering Solutions of Sandia, LLC., a wholly owned subsidiary of Honeywell International, Inc., for the U.S. Department of Energy's National Nuclear Security Administration under contract DE-NA0003525. EB and AT contributed to this work as part of their summer internship at Sandia National Laboratories, supported by the National

Science Foundation under award EAR-1852339 and the NSF GAGE and SAGE facilities, operated by EarthScope.

Institutional Review Board Statement: Not applicable.

Informed Consent Statement: Not applicable.

Data Availability Statement: The full dataset described here is available on the open access repository Zenodo, https://doi.org/10.5281/zenodo.15868512.

Acknowledgments: The authors gratefully acknowledge P. G. Brown (WMPG, Western University) for his support and valuable contributions towards the compilation and release of this dataset. Sandia National Laboratories is a multi-mission laboratory managed and operated by National Technology and Engineering Solutions of Sandia, LLC (NTESS), a wholly owned subsidiary of Honeywell International Inc., for the U.S. Department of Energy's National Nuclear Security Administration (DOE/NNSA) under contract DE-NA0003525. This written work is authored by an employee of NTESS. The employee, not NTESS, owns the right, title, and interest in and to the written work and is responsible for its contents. Any subjective views or opinions that might be expressed in the written work do not necessarily represent the views of the U.S. Government. The publisher acknowledges that the U.S. Government retains a non-exclusive, paid-up, irrevocable, world-wide license to publish or reproduce the published form of this written work or allow others to do so, for U.S. Government purposes. The DOE will provide public access to results of federally sponsored research in accordance with the DOE Public Access Plan. This material is based upon work supported by the National Science Foundation under award EAR-1852339 and the NSF GAGE and SAGE facilities, operated by EarthScope. Any opinions, findings, and conclusions or recommendations expressed in this material are those of the author(s) and do not necessarily reflect the views of the National Science Foundation.

Conflicts of Interest: The authors declare no conflicts of interest.

Notes

[1] https://github.com/obspy/obspy/wiki/ (accessed on 25 June 2025)
[2] https://github.com/obspy/obspy/wiki/ (accessed on 25 June 2025)
[3] https://earthquakescanada.nrcan.gc.ca/fdsnws (accessed on 25 June 2025)

References

1. Silber, E.A. *Observational and Theoretical Investigation of Cylindrical Line Source Blast Theory Using Meteors*; Western University: London, ON, Canada, 2014.
2. Silber, E.A.; Brown, P.G. Optical observations of meteors generating infrasound—I: Acoustic signal identification and phenomenology. *J. Atmos. Sol.-Terr. Phys.* **2014**, *119*, 116–128. [CrossRef]
3. Edwards, W.N.; Brown, P.G.; Weryk, R.J.; ReVelle, D.O. Infrasonic Observations of Meteoroids: Preliminary Results from a Coordinated Optical-radar-infrasound Observing Campaign. In *Advances in Meteoroid and Meteor Science*; Trigo-Rodríguez, J.M., Rietmeijer, F.J.M., Llorca, J., Janches, D., Eds.; Springer: New York, NY, USA, 2008; pp. 221–229.
4. De Groot-Hedlin, C.D.; Hedlin, M.A.H.; Drob, D. Atmospheric variability and infrasound monitoring. In *Infrasound Monitoring for Atmospheric Studies*; Le Pichon, A., Blanc, E., Hauchecorne, A., Eds.; Springer: Berlin/Heidelberg, Germany, 2010.
5. Drob, D.P.; Picone, J.M.; Garces, M. Global morphology of infrasound propagation. *J. Geophys. Res.* **2003**, *108*, 1–12. [CrossRef]
6. Nishikawa, Y.; Yamamoto, M.-Y.; Sansom, E.K.; Devillepoix, H.A.R.; Towner, M.C.; Hiramatsu, Y.; Kawamura, T.; Fujita, K.; Yoshikawa, M.; Ishihara, Y.; et al. Modeling of 3D trajectory of Hayabusa2 re-entry based on acoustic observations. *Publ. Astron. Soc. Jpn.* **2022**, *74*, 308–317. [CrossRef]
7. Silber, E.; Bowman, D.C. Along-trajectory acoustic signal variations observed during the hypersonic reentry of the OSIRIS-REx Sample Return Capsule. *Seismol. Res. Lett.* **2025**, *96*, 2767–2779. [CrossRef]
8. Pilger, C.; Gaebler, P.; Hupe, P.; Ott, T.; Drolshagen, E. Global Monitoring and Characterization of Infrasound Signatures by Large Fireballs. *Atmosphere* **2020**, *11*, 83. [CrossRef]
9. Ens, T.A.; Brown, P.G.; Edwards, W.N.; Silber, E.A. Infrasound production by bolides: A global statistical study. *J. Atmos. Sol.-Terr. Phys.* **2012**, *80*, 208–229. [CrossRef]

10. Silber, E.A.; Trigo-Rodriguez, J.; Oseghae, I.; Peña Asensio, E.; Boslough, M.B.; Whitaker, R.; Pilger, C.; Lubin, P.; Sawal, V.; Hetzer, C.; et al. Multiparameter constraints on empirical infrasound period–yield relations for bolides and implications for planetary defense. *Astron. J.* **2025**, *170*, 38. [CrossRef]
11. Gi, N.; Brown, P. Refinement of bolide characteristics from infrasound measurements. *Planet. Space Sci.* **2017**, *143*, 169–181. [CrossRef]
12. Bowman, D.C.; Silber, E.A.; Giannone, M.R.; Albert, S.A.; Edwards, T.; Dugick, F.K.D.; Longenbaugh, R.S. Acoustic Waves from the 20 April 2023 SpaceX Starship Rocket Explosion Traveling in the Elevated 'AtmoSOFAR' Channel. *Geophys. J. Int.* **2025**, *241*, 1053–1065. [CrossRef]
13. Pilger, C.; Ceranna, L.; Ross, J.O.; Le Pichon, A.; Mialle, P.; Garcés, M.A. CTBT infrasound network performance to detect the 2013 Russian fireball event. *Geophys. Res. Lett.* **2015**, *42*, 2523–2531. [CrossRef]
14. Brown, P.; McCausland, P.J.A.; Fries, M.; Silber, E.; Edwards, W.N.; Wong, D.K.; Weryk, R.J.; Fries, J.; Krzeminski, Z. The fall of the Grimsby meteorite—I: Fireball dynamics and orbit from radar, video, and infrasound records. *Meteorit. Planet. Sci.* **2011**, *46*, 339–363. [CrossRef]
15. Brown, P.G.; McCausland, P.J.A.; Hildebrand, A.R.; Hanton, L.T.J.; Eckart, L.M.; Busemann, H.; Krietsch, D.; Maden, C.; Welten, K.; Caffee, M.W.; et al. The Golden meteorite fall: Fireball trajectory, orbit, and meteorite characterization. *Meteorit. Planet. Sci.* **2023**, *58*, 1773–1807. [CrossRef]
16. Borovička, J.; Tóth, J.; Igaz, A.; Spurný, P.; Kalenda, P.; Haloda, J.; Svoreň, J.; Kornoš, L.; Silber, E.; Brown, P.; et al. The Košice meteorite fall: Atmospheric trajectory, fragmentation, and orbit. *Meteorit. Planet. Sci.* **2013**, *48*, 1757–1779. [CrossRef]
17. Brown, P.; ReVelle, D.O.; Tagliaferri, E.; Hildebrand, A.R. An entry model for the Tagish Lake fireball using seismic, satellite and infrasound records. *Meteorit. Planet. Sci.* **2002**, *37*, 661–675. [CrossRef]
18. Silber, E.A. Perspectives and Challenges in Bolide Infrasound Processing and Interpretation: A Focused Review with Case Studies. *Remote Sens.* **2024**, *16*, 3628. [CrossRef]
19. Silber, E.A.; Brown, P.G.; Krzeminski, Z. Optical observations of meteors generating infrasound: Weak shock theory and validation. *J. Geophys. Res. Planets* **2015**, *120*, 413–428. [CrossRef]
20. Beyreuther, M.; Barsch, R.; Krischer, L.; Megies, T.; Behr, Y.; Wassermann, J. ObsPy: A Python toolbox for seismology. *Seismol. Res. Lett.* **2010**, *81*, 530–533. [CrossRef]
21. Krischer, L.; Megies, T.; Barsch, R.; Beyreuther, M.; Lecocq, T.; Caudron, C.; Wassermann, J. ObsPy: A bridge for seismology into the scientific Python ecosystem. *Comput. Sci. Discov.* **2015**, *8*, 014003. [CrossRef]
22. Megies, T.; Beyreuther, M.; Barsch, R.; Krischer, L.; Wassermann, J. ObsPy–What can it do for data centers and observatories? *Ann. Geophys.* **2011**, *54*, 47–58. [CrossRef]
23. Brown, P.; Weryk, R.J.; Kohut, S.; Edwards, W.N.; Krzemenski, Z. Development of an All-Sky Video Meteor Network in Southern Ontario, Canada: The ASGARD System. *WGN J. Int. Meteor Organ.* **2010**, *38*, 25–30.
24. Weryk, R.; Brown, P.; Domokos, A.; Edwards, W.; Krzeminski, Z.; Nudds, S.; Welch, D. The Southern Ontario all-sky meteor camera network. *Earth Moon Planets* **2008**, *102*, 241–246. [CrossRef]
25. Weryk, R.; Campbell-Brown, M.; Wiegert, P.; Brown, P.; Krzeminski, Z.; Musci, R. The Canadian automated meteor observatory (CAMO): System overview. *Icarus* **2013**, *225*, 614–622. [CrossRef]
26. Weryk, R.J.; Brown, P.G. Simultaneous radar and video meteors—I: Metric comparisons. *Planet. Space Sci.* **2012**, *62*, 132–152. [CrossRef]
27. Weryk, R.J.; Brown, P.G. Simultaneous radar and video meteors—II: Photometry and ionisation. *Planet. Space Sci.* **2013**, *81*, 32–47. [CrossRef]
28. Swinbank, R.; O'Neill, A.A. Stratosphere-troposphere data assimilation system. *Mon. Weather Rev.* **1994**, *122*, 686–702. [CrossRef]
29. Drob, D.P.; Emmert, J.T.; Crowley, G.; Picone, J.M.; Shepherd, G.G.; Skinner, W.; Hays, P.; Niciejewski, R.J.; Larsen, M.; She, C.Y.; et al. An empirical model of the Earth's horizontal wind fields: HWM07. *J. Geophys. Res.* **2008**, *113*, A12304. [CrossRef]
30. Hetzer, C.H. The NCPAG2S Command Line Client. 2024. Available online: https://github.com/chetzer-ncpa/ncpaprop-release (accessed on 3 June 2025).
31. Antier, K.; Le Pichon, A.; Vergniolle, S.; Zielinski, C.; Lardy, M. Multiyear validation of the NRL-G2S wind fields using infrasound from Yasur. *J. Geophys. Res. Atmos.* **2007**, *112*, 1–6. [CrossRef]
32. Schwaiger, H.F.; Iezzi, A.M.; Fee, D. AVO-G2S: A modified, open-source Ground-to-Space atmospheric specification for infrasound modeling. *Comput. Geosci.* **2019**, *125*, 90–97. [CrossRef]
33. Silber, E.A.; Boslough, M.; Hocking, W.K.; Gritsevich, M.; Whitaker, R.W. Physics of meteor generated shock waves in the Earth's atmosphere—A review. *Adv. Space Res.* **2018**, *62*, 489–532. [CrossRef]
34. Ceplecha, Z.; Borovička, J.; Elford, W.G.; ReVelle, D.O.; Hawkes, R.L.; Porubčan, V.; Šimek, M. Meteor Phenomena and Bodies. *Space Sci. Rev.* **1998**, *84*, 327–471. [CrossRef]
35. Bronshten, V.A. *Physics of Meteoric Phenomena*; D. Reidel Publishing Co.: Dordrecht, The Netherlands, 1983.

36. Tsikulin, M. *Shock Waves During the Movement of Large Meteorites in the Atmosphere*; DTIC Document AD 715-537; National Technical Information Service: Springfield, VA, USA, 1970.
37. ReVelle, D.O. On meteor-generated infrasound. *J. Geophys. Res.* **1976**, *81*, 1217–1230. [CrossRef]
38. Silber, E.A.; Brown, P. Infrasound Monitoring as a Tool to Characterize Impacting Near-Earth Objects (NEOs). In *Infrasound Monitoring for Atmospheric Studies: Challenges in Middle Atmosphere Dynamics and Societal Benefits*; Le Pichon, A., Blanc, E., Hauchecorne, A., Eds.; Springer International Publishing: Cham, Switzerland, 2019; pp. 939–986.
39. Brown, P.; Edwards, W.; ReVelle, D.; Spurny, P. Acoustic analysis of shock production by very high-altitude meteors—I: Infrasonic observations, dynamics and luminosity. *J. Atmos. Sol.-Terr. Phys.* **2007**, *69*, 600–620. [CrossRef]
40. Trigo-Rodríguez, J.M.; Dergham, J.; Gritsevich, M.; Lyytinen, E.; Silber, E.A.; Williams, I.P. A Numerical Approach to Study Ablation of Large Bolides: Application to Chelyabinsk. *Adv. Astron.* **2021**, *2021*, 8852772. [CrossRef]
41. Edwards, W.N. Meteor Generated Infrasound: Theory and Observation. In *Infrasound Monitoring for Atmospheric Studies*; Le Pichon, A., Blanc, E., Hauchecorne, A., Eds.; Springer: Dordrecht, The Netherlands, 2009; pp. 361–414.
42. Plooster, M.N. Shock Waves from Line Sources. Numerical Solutions and Experimental Measurements. *Phys. Fluids* **1970**, *13*, 2665–2675. [CrossRef]
43. Wilson, T.C.; Silber, E.A.; Colston, T.A.; Elbing, B.R.; Edwards, T.R. Bolide infrasound signal morphology and yield estimates: A case study of two events detected by a dense acoustic sensor network. *Astron. J.* **2025**, *169*, 223. [CrossRef]
44. Evans, L.B.; Bass, H.E.; Sutherland, L.C. Atmospheric Absorption of Sound: Theoretical Predictions. *J. Acoust. Soc. Am.* **1972**, *51*, 1565–1575. [CrossRef]
45. Silber, E.A.; Bowman, D.C. Isolating the Source Region of Infrasound Travel Time Variability Using Acoustic Sensors on High-Altitude Balloons. *Remote Sens.* **2023**, *15*, 3661. [CrossRef]
46. Kromer, R.P.; McDonald, T.S. Infrasound Sensor Models And Evaluation. In Proceedings of the 22nd Annual DoD/DOE Seismic Research Symposium, New Orleans, LA, USA, 13–15 September 2000.
47. Alcoverro, B.; Le Pichon, A. Design and optimization of a noise reduction system for infrasonic measurements using elements with low acoustic impedance. *J. Acoust. Soc. Am.* **2005**, *117*, 1717–1727. [CrossRef] [PubMed]
48. Christie, D.R.; Campus, P. The IMS infrasound network: Design and establishment of infrasound stations. In *Infrasound Monitoring for Atmospheric Studies*; Springer: Berlin/Heidelberg, Germany, 2010; pp. 29–75.